

Adsorption of C₂H Radical on Cobalt Clusters: Anion Photoelectron Spectroscopy and Density Functional Calculations

Jinyun Yuan, Hong-Guang Xu, Zeng-Guang Zhang, Yuan Feng, and Weijun Zheng*

Beijing National Laboratory for Molecular Sciences, State Key Laboratory of Molecular Reaction Dynamics, Institute of Chemistry, Chinese Academy of Sciences, Beijing 100190, China

Received: September 16, 2010; Revised Manuscript Received: November 10, 2010

We investigated the adsorption of C₂H radical on small cobalt clusters by mass spectrometry and by measuring the photoelectron spectra of Co_nC₂H[−] (*n* = 1–5) cluster anions. The most stable structures of Co_nC₂H[−] (*n* = 1–5) and their neutrals were determined by comparing the experimental results with theoretical calculations. Our studies show that C₂H radical still maintains its integrity as a structural unit in Co_nC₂H[−] clusters, rather than being divided by Co_n clusters. The most stable isomers of Co_{1–2}C₂H[−] clusters are linear with the C₂H interacting with only one Co atom, while those of Co_{3–5}C₂H[−] cluster anions are quasi-planar structures with the carbon–carbon bonds bending slightly toward the Co_{3–5} clusters. The carbon–carbon bond of C₂H is lengthened more in Co_{3–5}C₂H[−] clusters than in Co_{1–2}C₂H[−].

1. Introduction

The ethynyl radical (C₂H) is a widespread interstellar molecule which has been detected in a variety of sources, such as planetary nebulae,^{1,2} molecular clouds,^{3,4} and star-forming regions.^{5,6} It is also an important reactive intermediate in hydrocarbon combustion processes.^{7–9} In past decades, a great deal of effort has been devoted to studying the C₂H radical.^{10–20} Lineberger and co-workers measured the photoelectron spectrum of C₂H and determined the electron affinity (EA) of C₂H to be 2.97 eV.¹³ Wu and Cheng reported the infrared absorption spectra of C₂H radicals isolated in solid neon.¹⁴ Tarroni and Carter calculated the rovibronic levels for the X ²Σ and A ²Π electronic states of C₂H¹⁷ and reported the energies, rotational constants, and spin–orbit splittings of all levels of Σ, Π, Δ, and Φ symmetry up to 6400 cm^{−1} for C₂H. Neumark and co-workers investigated C₂H and C₂D radicals by slow electron velocity-map imaging of the corresponding anions.¹⁹

Understanding the interactions between metal and organic molecules is important in both heterogeneous and homogeneous catalytic systems. Consequently, experimental and theoretical works were conducted to study the complexes formed between metal atoms and C₂H radical. Brugh et al.²¹ measured the vibronic spectrum of CrC₂H at the 11 100–13 300 cm^{−1} region and showed that the CrC₂H molecule has a linear structure in both the ground and excited states. Looock et al. determined the frequencies of the Yb–C stretching mode and Yb–C–C bending mode of YbC₂H by combination of resonance-enhanced two photon ionization, laser-induced fluorescence, and photoionization efficiency spectroscopy experiments with DFT calculations.²² Bernath and co-workers analyzed the gas-phase free radicals CaC₂H and SrC₂H by laser excitation spectroscopy and laser-induced fluorescence.^{23,24} The pure rotational spectra of NaC₂H, MgC₂H, CaC₂H, and SrC₂H were measured by Ziurys and co-workers using millimeter/submillimeter direct absorption spectroscopy.^{25–28} The photoelectron spectrum of FeC₂H[−] has been reported by Wang and co-workers;²⁹ that of PdC₂H[−] has been reported by Jarrold and co-workers.³⁰

The studies in the literature are mainly focused on the interaction of C₂H radical with one metal atom. In this work, we report a study on the adsorption of C₂H radical on small Co_n (*n* = 1–5) clusters in the gas phase by anion photoelectron spectroscopy (PES) and density functional theory (DFT) calculations. It is known that cobalt has a high affinity to carbon–carbon π-bonds. Cobalt is an essential catalyst constituent in many organic reactions.^{31–34} Hence, it would be interesting to investigate the interaction between C₂H radical and cobalt clusters.

2. Experimental and Theoretical Methods

2.1. Experimental Methods. The experiments were conducted on a home-built apparatus consisting of a time-of-flight mass spectrometer and a magnetic bottle photoelectron spectrometer, which has been described elsewhere.³⁵ The Co_nC₂H[−] (*n* = 1–5) cluster anions were generated in a laser vaporization source in which a rotating, translating cobalt target (13 mm diameter) was ablated with the second harmonic (532 nm, 2.331 eV) of a Nd:YAG laser (Continuum Surelite II-10) while helium gas with ~4 atm pressure seeded with ethene molecules (~1%) was allowed to expand through a pulsed valve over the cobalt target. The cluster anions were mass-analyzed by the time-of-flight mass spectrometer. The Co_nC₂H[−] (*n* = 1–5) clusters were mass-selected and decelerated before being photodetached. The selected cluster anions were photodetached using the second harmonic and the fourth harmonic (266 nm, 4.661 eV) of the Nd:YAG laser, respectively. The resulted electrons were energy-analyzed by the magnetic bottle photoelectron spectrometer. The PES spectra were calibrated using the known spectra of Cu[−] and Co[−]. The instrumental resolution was approximately 40 meV for electrons with 1 eV kinetic energy.

2.2. Theoretical Methods. The geometry optimizations of Co_nC₂H[−] (*n* = 1–5) were carried out by the density functional theory (DFT) with B3LYP^{36–39} exchange–correlation potential. The various structures were calculated by using 6-311+G(d,p) basis sets for C and H atoms and LanL2DZ basis set for Co atom. All geometry optimizations were conducted without any symmetry constraint, and the calculated energies were corrected by zero-point vibrational energies. Harmonic vibrational fre-

* Corresponding author. E-mail: zhengwj@iccas.ac.cn.

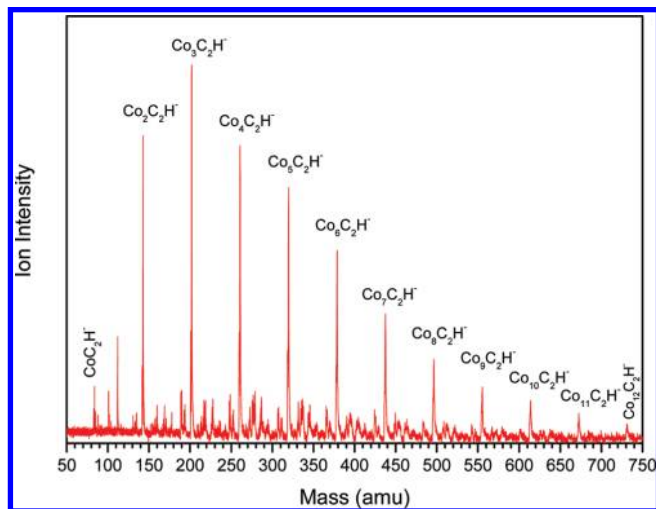


Figure 1. Mass spectrum of $\text{Co}_n\text{C}_2\text{H}^-$ ($n = 1-12$) cluster anions.

quencies were calculated to make sure that the structures correspond to real local minima. We also calculated the S^2 values of each isomer to make sure that the spin contaminations are negligible. All theoretical calculations were performed with the Gaussian 03 program package.⁴⁰

3. Experimental Results

Figure 1 shows a typical mass spectrum of cluster anions generated in our experiment. It can be seen that the predominant mass peaks are those of $\text{Co}_n\text{C}_2\text{H}^-$ cluster anions. We are able to observe the cluster size of $\text{Co}_n\text{C}_2\text{H}^-$ up to $n = 12$.

The photoelectron spectra of $\text{Co}_n\text{C}_2\text{H}^-$ ($n = 1-5$) measured with 532 and 266 nm photons are shown in Figure 2. The vertical detachment energies (VDEs) and the adiabatic detachment energies (ADEs) of $\text{Co}_n\text{C}_2\text{H}^-$ ($n = 1-5$) cluster anions estimated from their photoelectron spectra are summarized in Table 1. The EAs of $\text{Co}_{1-5}\text{C}_2\text{H}$ are in the range 1.19–1.73 eV, much lower than that of C_2H (2.97 eV),^{13,19} implying that cobalt atoms play an important role in the PES features of $\text{Co}_n\text{C}_2\text{H}^-$ ($n = 1-5$).

3.1. CoC_2H^- . The photoelectron spectrum of CoC_2H^- (Figure 2) at 266 nm has two major features centered at 1.3 and 1.9 eV. Some weak features are discernible at electron binding energy higher than 2.0 eV. More details of the low binding energy features can be distinguished in the spectrum taken at 532 nm. In the spectrum at 532 nm, we can see the first feature is composed of four small peaks at 1.19, 1.25, 1.31, and 1.37 eV, which probably correspond to the vibrational states of CoC_2H neutral. The vibrational frequency is estimated to be $480 \pm 80 \text{ cm}^{-1}$ based on the space between those peaks. The position of the 1.9 eV feature in the 266 nm spectrum is determined more precisely to be $\sim 1.86 \text{ eV}$ at 532 nm. The relative intensities of the two features are different between the spectra at 532 and 266 nm. That is probably due to the different electron detachment cross sections at different wavelengths. The electron affinity of CoC_2H is estimated to be $\sim 1.19 \text{ eV}$, much lower than that of CoC_2 (1.70 eV).⁴¹ It is analogous with the cases of C_2 and C_2H that addition of a hydrogen atom to C_2 reduces the electron affinity, as it was shown by Lineberger and co-workers that the EA of C_2 is 3.27 eV while it is 2.97 eV for C_2H .¹³

3.2. $\text{Co}_2\text{C}_2\text{H}^-$. The photoelectron spectrum of $\text{Co}_2\text{C}_2\text{H}^-$ (Figure 2) taken with 266 nm photons reveals three intense features centered at 1.50, 2.26, and 3.25 eV. The band centered

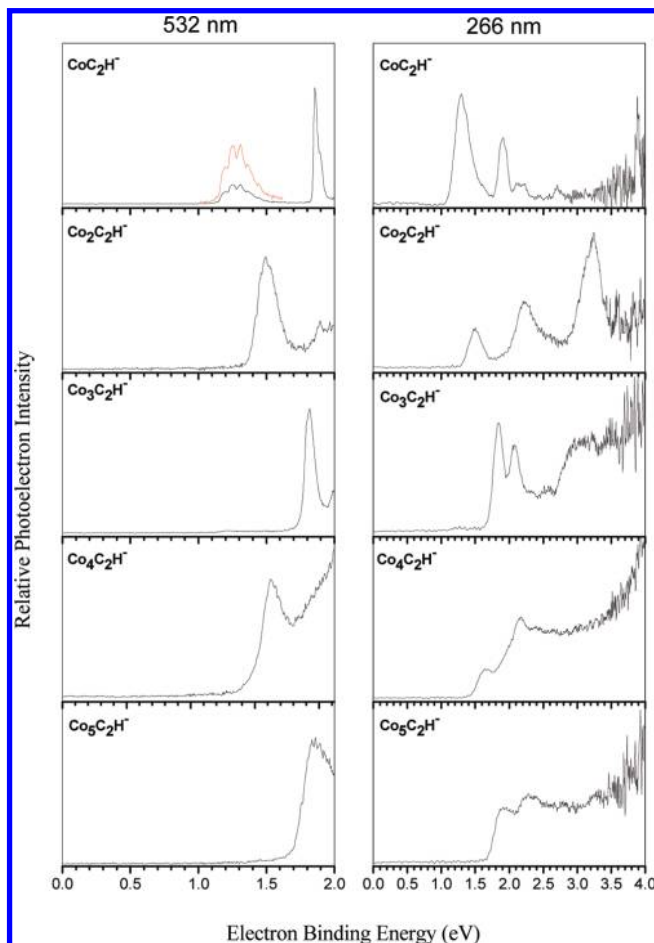


Figure 2. Photoelectron spectra of $\text{Co}_n\text{C}_2\text{H}^-$ ($n = 1-5$) cluster anions recorded with 532 and 266 nm photons.

TABLE 1: Experimentally Observed VDEs and ADEs from the Photoelectron Spectra of $\text{Co}_n\text{C}_2\text{H}^-$ ($n = 1-5$)^a

cluster	VDE (eV)	ADE (eV)
CoC_2H^-	1.25(8)	1.19(8)
$\text{Co}_2\text{C}_2\text{H}^-$	1.50(8)	1.39(8)
$\text{Co}_3\text{C}_2\text{H}^-$	1.81(8)	1.73(8)
$\text{Co}_4\text{C}_2\text{H}^-$	1.63(8)	1.42(8)
$\text{Co}_5\text{C}_2\text{H}^-$	1.88(8)	1.69(8)

^a The numbers in parentheses indicate the uncertainties in the last digit.

at 1.50 eV is also observed in the spectrum of $\text{Co}_2\text{C}_2\text{H}^-$ at 532 nm. We note that there is a tiny peak at 1.89 eV in the spectrum at 532 nm. That peak is not so clear in the 266 nm spectrum due to the low resolution and the background noise at that wavelength. The EA of $\text{Co}_2\text{C}_2\text{H}$ is estimated to be 1.39 eV, lower than that of Co_2C_2 ($1.6 \pm 0.15 \text{ eV}$).⁴²

3.3. $\text{Co}_3\text{C}_2\text{H}^-$. The photoelectron spectrum of $\text{Co}_3\text{C}_2\text{H}^-$ (Figure 2) at 266 nm exhibits two well-resolved peaks centered at 1.85 and 2.09 eV and followed by several unresolved broad peaks at the higher binding energy. The spectrum at 532 nm shows better resolution for the first peak. Thus, we are able to determine the position of that peak more precisely to be 1.81 eV. That peak is relatively sharp, suggesting that there is little geometry change between the ground state of the anion and that of the neutral. The EA of $\text{Co}_3\text{C}_2\text{H}$ is estimated to be about 1.73 eV.

3.4. $\text{Co}_4,5\text{C}_2\text{H}^-$. The spectral features of $\text{Co}_4\text{C}_2\text{H}^-$ and $\text{Co}_5\text{C}_2\text{H}^-$ (Figure 2) are broad. In their spectra at 266 nm, we could only distinguish two peaks centered at ~ 1.65 and 2.17

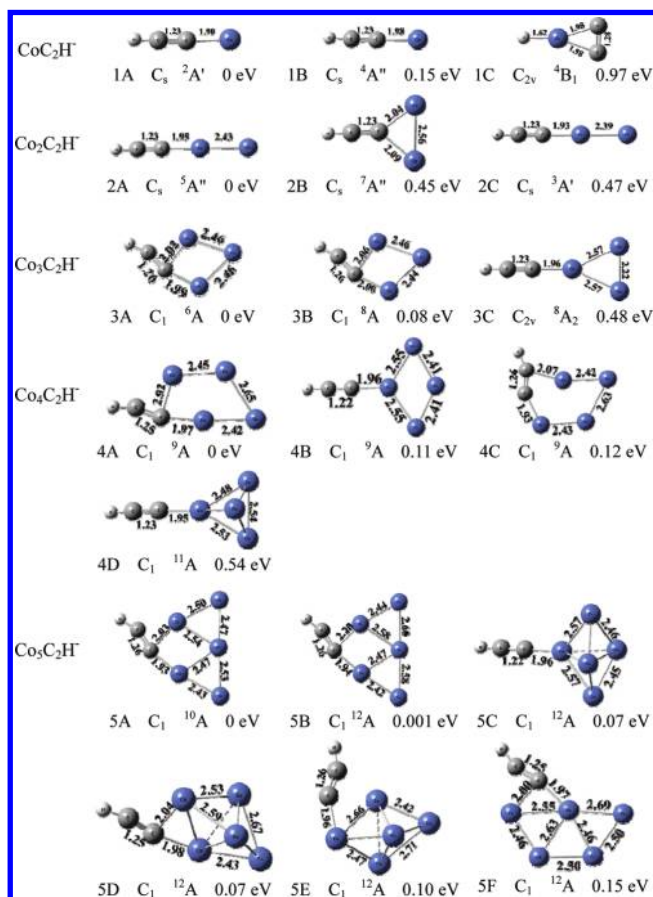


Figure 3. Optimized geometries of low-lying isomers of $\text{Co}_n\text{C}_2\text{H}^-$ ($n = 1-5$).

eV for $\text{Co}_4\text{C}_2\text{H}^-$ and two peaks at ~ 1.93 and 2.31 eV for $\text{Co}_5\text{C}_2\text{H}^-$. Since the 532 nm spectra show better resolution, we could determine the VDEs of $\text{Co}_4\text{C}_2\text{H}^-$ and $\text{Co}_5\text{C}_2\text{H}^-$ to be 1.63 and 1.88 eV respectively based on their 532 nm spectra. The EAs of $\text{Co}_4\text{C}_2\text{H}$ and $\text{Co}_5\text{C}_2\text{H}$ are estimated to be ~ 1.42 eV and ~ 1.69 eV, respectively.

4. Theoretical Results and Discussion

The optimized geometries of the low-lying isomers of $\text{Co}_n\text{C}_2\text{H}^-$ ($n = 1-5$) cluster anions obtained with DFT calculations are presented in Figure 3 with the most stable structures on the left. We have considered many spin multiplicities and various initial structures, such as to insert Co atoms between the two carbon atoms or between the C and H atoms. However, those tried geometries are less stable than the structures with C_2H attached directly to Co_n ($n = 1-5$) clusters. The fact indicates that the C_2H is a stable unit. The calculations show that the most stable structures of $\text{Co}_n\text{C}_2\text{H}^-$ ($n = 1-5$) cluster anions are all planar or quasi-planar structures.

The structures of the neutral clusters $\text{Co}_n\text{C}_2\text{H}$ ($n = 1-5$) were also optimized using their corresponding anion structures in Figure 3 as initial structures. The most stable structures of $\text{Co}_n\text{C}_2\text{H}$ ($n = 1-5$) neutrals are presented in Figure 4. We found that the neutral structures vary only slightly from their corresponding anions. Based on the energy differences between the neutrals and anions, we calculated the ADEs of these isomers (EAs of the neutrals). The calculated VDEs and ADEs of $\text{Co}_n\text{C}_2\text{H}^-$ ($n = 1-5$) cluster anions are listed in Table 2, in which the experimental values are also presented.

4.1. CoC_2H^- . For CoC_2H^- , the isomer with the lowest energy is 1A (Figure 3 and Table 2), which is a linear structure

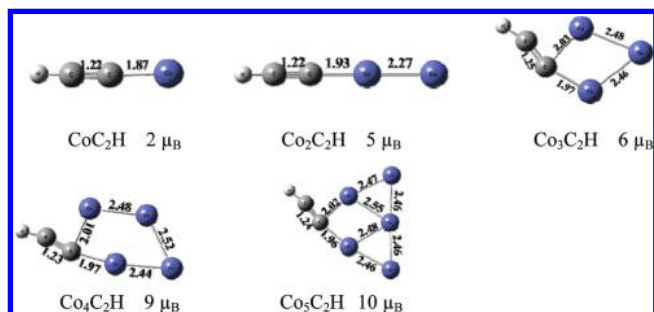


Figure 4. Optimized geometries of the most stable isomers of neutral $\text{Co}_n\text{C}_2\text{H}$ ($n = 1-5$).

TABLE 2: Relative Energies of the Lower Energy Isomers of $\text{Co}_n\text{C}_2\text{H}^-$ ($n = 1-5$) As Well As Their VDEs and ADEs Obtained by DFT Calculations

cluster	state	ΔE (eV)	VDE (eV)		ADE (eV)	
			theor	expt	theor	expt
CoC ₂ H ⁻	1A $^2\text{A}'$	0	1.10	1.25	1.09	1.19
	1B $^4\text{A}''$	0.15	1.01		0.94	
	1C $^4\text{B}_1$	0.97	3.77		3.29	
Co ₂ C ₂ H ⁻	2A $^5\text{A}''$	0	1.53	1.50	1.42	1.39
	2B $^7\text{A}''$	0.45	2.23		1.14	
	2C $^3\text{A}'$	0.47	1.42		1.29	
Co ₃ C ₂ H ⁻	3A ^6A	0	1.59	1.81	1.56	1.73
	3B ^8A	0.08	1.91		1.57	
	3C $^8\text{A}_2$	0.48	1.42		0.79	
Co ₄ C ₂ H ⁻	4A ^9A	0	1.82	1.63	1.54	1.42
	4B ^9A	0.11	2.17		1.44	
	4C ^9A	0.12	1.77		1.42	
	4D ^{11}A	0.54	2.08		1.01	
Co ₅ C ₂ H ⁻	5A ^{10}A	0	2.15	1.88	1.86	1.69
	5B ^{12}A	0.001	2.37		2.20	
	5C ^{12}A	0.07	2.30		1.91	
	5D ^{12}A	0.07	2.02		1.85	
	5E ^{12}A	0.10	2.08		1.83	
	5F ^{12}A	0.15	2.13		1.99	

with C_s symmetry and $^2\text{A}'$ ground electronic state. The Co atom attaches to the terminal C atom of C_2H in isomer 1A. The C–C distance is 1.23 \AA , slightly longer than the $\text{C}\equiv\text{C}$ bond of acetylene (1.20 \AA)⁴³ but much shorter than the $\text{C}=\text{C}$ bond (1.33 \AA) of ethene.⁴⁴ The C–Co bond is 1.90 \AA , 0.04 \AA longer than that of CoC_2^- anion (1.86 \AA).⁴² The calculated VDE (1.10 eV) of isomer 1A is in agreement with the experimental measurement (1.25 eV). The second most stable isomer (1B) is also a linear structure similar to 1A but in the quartet state. The energy of isomer 1B lies 0.15 eV above isomer 1A, and the calculated VDE is also consistent with the experimental value. However, the theoretical ADE and VDE of isomer 1A are much closer to the experimental values than those of isomer 1B. Thus, isomer 1A might be the major structure and isomer 1B is possibly the minor structure generated in the experiments. Isomer 1C is 0.97 eV higher in energy than isomer 1A, and its theoretical value of VDE is inconsistent with the experimental value. Therefore, the existence of isomer 1C in our experiments can be ruled out. Our calculations show that the frequency of the Co–C bond stretching mode of CoC_2H neutral is about 462 cm^{-1} . That is consistent with the experimental value ($480 \pm 80 \text{ cm}^{-1}$) estimated from the photoelectron spectrum. The Co–C stretching mode of CoC_2H neutral is close to the Cr–C stretching (470 cm^{-1}) and Fe–C stretching (500 cm^{-1}) modes of $\text{CrC}_2\text{H}^{21}$ and $\text{FeC}_2\text{H}^{29}$ which also have linear structures.

4.2. $\text{Co}_2\text{C}_2\text{H}^-$. The most stable isomer (2A; Figure 3 and Table 2) of $\text{Co}_2\text{C}_2\text{H}^-$ is a linear structure in the $^5\text{A}''$ state. Isomer 2A is formed by attaching a Co atom to CoC_2H^- via a Co–Co

bond. The C–C bond is also 1.23 Å, the same as that in CoC₂H⁻. The C–Co bond is 1.95 Å, 0.05 Å longer than that in CoC₂H⁻. The Co–Co bond is 2.43 Å, which is very close to the Co–Co bond in the bare Co₂ cluster (2.36–2.44 Å).⁴⁵ The calculated ADE and VDE of isomer 2A are 1.42 and 1.53 eV, respectively, which are consistent with those measured from the PES spectra (1.39, 1.50 eV). The next most stable isomer (2B) is a triangular structure in the septet state in which the C–C bond is also 1.23 Å. The calculated VDE of isomer 2B (2.23 eV) is much higher than the experimental value. Isomer 2C is in the triplet state. It also has a linear structure similar to isomer 2A, and its theoretical ADE and VDE are close to the experimental values. However, it is 0.47 eV higher in energy than isomer 2A. Therefore, we suggest that isomer 2A is the major one contributing to the experimental PES features of Co₂C₂H⁻.

4.3. Co₃C₂H⁻. The ground state structure of bare Co₃ cluster is calculated to be a triangular structure^{46–50} or a linear structure^{51,52} by different research groups. Yoshida et al.⁵³ reported Co₃⁻ cluster anion to be linear with Co–Co distances of 2.25–2.50 Å based on photoelectron spectroscopy and theoretical calculations. Our calculations show that the three Co atoms in Co₃C₂H⁻ form a triangle. The first two isomers of Co₃C₂H⁻, isomers 3A and 3B, are very close in energy and geometry (see Figure 3 and Table 2). The Co₃ cluster in 3A is an isosceles triangle structure, while that in 3B is slightly distorted. Isomer 3A is in the ⁶A state, while isomer 3B is in the ⁸A state. Isomer 3B is higher in energy than isomer 3A by only 0.08 eV. These two lowest energy structures are formed by adding the C₂H to the Co₃ cluster with two Co atoms attached to the terminal C atom of C₂H forming a four-member ring. The C–C bonds of isomers 3A and 3B are both 1.26 Å, 0.03 Å longer than those in Co_{1–2}C₂H⁻. The theoretical VDEs and ADEs of isomers 3A and 3B are both close to the experimental values (1.81, 1.73 eV). Therefore, we suggest that isomers 3A and 3B coexist in the experiments. The existence of isomer 3C can be excluded since its energy is 0.48 eV higher than isomer 3A and its VDE and ADE deviate much from the experimental values.

4.4. Co₄C₂H⁻. The ground state structure of bare Co₄ cluster by theoretical calculations also varies in the literature. It has been reported to be a distorted tetrahedral structure,⁴⁸ a planar rhombus structure,^{51,54} or an out-of-plane rhombus structure.^{49,50,52} Yoshida et al.⁵³ suggested that the Co₄⁻ cluster anion has a tetrahedral structure based on photoelectron spectroscopy and theoretical calculations. We optimized the structures of Co₄C₂H⁻ by considering all possible geometries of Co₄ cluster reported in the literature. Our calculations show that the energy separation between the first two most stable isomers of Co₄C₂H⁻ (isomers 4A and 4B; see Figure 3) is only 0.11 eV. Isomer 4A has a five-member-ring structure which consists of a four-member ring of Co₄ cluster and the terminal carbon atom of C₂H. The C–C bond distance of isomer 4A is 1.25 Å, longer than the C≡C bond (1.20 Å) of acetylene⁴³ and shorter than the C=C bond (1.33 Å) of ethene.⁴⁴ Isomer 4B is a little out-of-plane rhombus structure in which the Co–Co bonds are 2.41 and 2.55 Å. Although isomer 4B is only 0.11 eV higher in energy than isomer 4A, its theoretical VDE (2.17 eV; Table 2) deviates much from the experimental value, indicating that its existence in the experiments can be ruled out. The calculated VDE of isomer 4A (1.82 eV) is consistent with our experimental value (1.63 eV). Therefore, isomer 4A is what we observed for Co₄C₂H⁻ in our experiment. Isomer 4C is only 0.12 eV higher than that of isomer 4A and its calculated ADE and VDE (1.42 and 1.77

eV) are in agreement with experimental measurements (1.42 and 1.63 eV). As a result, we suggest that both isomers 4A and 4C exist in our experiments, which explains why the bands in the spectra of Co₄C₂H⁻ are broad. Isomer 4D has a structure with C₂H attaching directly to one Co atom of a distorted tetrahedral Co₄ cluster. Isomer 4D is 0.54 eV higher in energy than isomer 4A. Its calculated VDE deviates much from those of the experimental measurement. As a result, the existence of isomer 4D in the experiments can be ruled out.

4.5. Co₅C₂H⁻. The bare Co₅ cluster has been reported to be a *D*_{3h} trigonal bipyramid,^{46,48,54,55} a *C*_{4v} square pyramid,⁴⁹ a *C*_{2v} rhombus pyramid,⁵¹ or a planar W-like structure⁵² by different theoretical calculations. Our calculations show that the first two low-lying isomers of Co₅C₂H⁻ at ¹⁰A and ¹²A states (5A and 5B), basically both contain planar W-like Co₅ units (Figure 3). They are very close in energy, with isomer 5B lying 0.001 eV above isomer 5A. The terminal C atom of C₂H radical connects to two Co atoms of the Co₅ unit. In these two isomers, the C–C bond distances are both 1.26 Å. Isomer 5C, 5D, and 5E are all composed of a distorted bipyramidal Co₅ unit and C₂H radical. Their energies lie 0.07, 0.07, and 0.10 eV above isomer 5A, respectively. Isomer 5F is also a structure consisted of a W-shaped Co₅ unit and C₂H which is 0.15 eV higher in energy than isomer 5A. Among of them, the calculated ADEs and VDEs of isomer 5A, 5D, 5E, and 5F are all close to the experimental values (Table 2), so they may all contribute to the PES features of Co₅C₂H⁻. That explains why the PES features of Co₅C₂H⁻ are broad.

In CoC₂H⁻ and Co₂C₂H⁻, the C₂H radical interacts with only one Co atom, and the C–C bond distances are estimated to be 1.23 Å, slightly longer than the C≡C bond of acetylene (1.20 Å)⁴³ but much shorter than the C=C bond (1.33 Å) of ethene.⁴⁴ This indicates that the C≡C bond of C₂H radical is only slightly affected by the Co and Co₂. In Co₃C₂H⁻, Co₄C₂H⁻, and Co₅C₂H⁻, the C₂H radical mainly interacts with two Co atoms, but there is also the possibility of interacting with only one Co atom. The carbon–carbon bonds bend toward the Co_{3–5} clusters. The C–C distances in Co_{3–5}C₂H⁻ are estimated to be 1.25–1.26 Å, which are between the C≡C and C=C bond lengths. Thus, the Co_{3–5} clusters have more effect on the C≡C bond of C₂H radical than those of Co and Co₂. The cobalt clusters might be useful for C≡C bond activation in organic synthesis.

4.6. Magnetic Properties. From Figure 4, we found that the magnetic moments of the most stable isomers of Co_{*n*}C₂H⁻ (*n* = 1–5) are 2μ_B, 5μ_B, 6μ_B, 9μ_B, and 10μ_B, respectively. These values are close to those of bare Co_{*n*} clusters. The magnetic moments of Co atom and Co_{*n*} (*n* = 2–5) clusters reported in the literature^{48,51,52} are 3μ_B, 4μ_B, 5μ_B (or 7μ_B), 8μ_B (or 10μ_B), and 11μ_B (or 13μ_B), respectively. That shows that adsorption of C₂H affects the magnetic moments of Co_{*n*} clusters only slightly. On the other hand, it has been reported that the chemisorbed benzene molecules affect the electronic structures of the cobalt clusters significantly, leading to the quench of their magnetic moments.⁵⁶ The difference is probably because the cobalt–benzene clusters form sandwich or rice-ball structures and thus the interaction between the π electrons of benzene molecules and cobalt d orbitals is very strong, while C₂H radical interacts with only one or two cobalt atoms through its terminal carbon atom.

5. Conclusions

We investigated the adsorption of C₂H radical on small cobalt clusters using anion photoelectron spectroscopy and DFT calculations. We found that C₂H radical is adsorbed to the cobalt

clusters through its terminal C atom. The terminal C atom interacts with one or two cobalt atoms of the cobalt clusters. The most stable isomers of $\text{Co}_{1-2}\text{C}_2\text{H}^-$ clusters are linear, and those of $\text{Co}_{3-5}\text{C}_2\text{H}^-$ cluster anions are quasi-planar structures. The C–C bond distances in $\text{Co}_{3-5}\text{C}_2\text{H}^-$ are longer than those in $\text{Co}_{1-2}\text{C}_2\text{H}^-$ clusters, indicating the larger Co clusters have more effect on the $\text{C}\equiv\text{C}$ bond of C_2H radical. The magnetic moments of Co_n ($n = 1-5$) clusters are only slightly influenced by the C_2H radical.

Acknowledgment. This work was supported by the Natural Science Foundation of China (NSFC, Grant 20933008). The theoretical calculations were conducted on the ScGrid and Deepcomp7000 the Supercomputing Center, Computer Network Information Center of Chinese Academy of Sciences.

References and Notes

- (1) Tucker, K. D.; Kutner, M. L.; Thaddeus, P. *Astrophys. J.* **1974**, *193*, L115.
- (2) Hasegawa, T. I.; Kwok, S. *Astrophys. J.* **2001**, *562*, 824.
- (3) Wootten, A.; Bozayan, E. P.; Garrett, D. B.; Loren, R. B.; Snell, R. L. *Astrophys. J.* **1980**, *239*, 844.
- (4) Lucas, R.; Liszt, H. S. *Astron. Astrophys.* **2000**, *358*, 1069.
- (5) Dutrey, A.; Guilloteau, S.; Guelin, M. *Astron. Astrophys.* **1997**, *317*, L55.
- (6) Beuther, H.; Semenov, D.; Henning, T.; Linz, H. *Astrophys. J.* **2008**, *675*, L33.
- (7) Kiefer, J. H.; Von Drasek, W. A. *Int. J. Chem. Kinet.* **1990**, *22*, 747.
- (8) Kiefer, J. H.; Sidhu, S. S.; Kern, R. D.; Xie, K.; Chen, H.; Harding, L. B. *Combust. Sci. Technol.* **1992**, *82*, 101.
- (9) Boullart, W.; Devriendt, K.; Borms, R.; Peeters, J. *J. Phys. Chem.* **1996**, *100*, 998.
- (10) Cochran, E. L.; Adrian, F. J.; Bowers, V. A. *J. Chem. Phys.* **1964**, *40*, 213.
- (11) Shepherd, R. A.; Graham, W. R. M. *J. Chem. Phys.* **1987**, *86*, 2600.
- (12) Chiang, W.-Y.; Hsu, Y.-C. *J. Chem. Phys.* **1999**, *111*, 1454.
- (13) Ervin, K. M.; Lineberger, W. C. *J. Phys. Chem.* **1991**, *95*, 1167.
- (14) Wu, Y.-J.; Cheng, B.-M. *Chem. Phys. Lett.* **2008**, *461*, 53.
- (15) Yan, W.-B.; Warner, H. E.; Amano, T. *J. Chem. Phys.* **1991**, *94*, 1712.
- (16) Yan, W.-B.; Amano, T. *J. Chem. Phys.* **1993**, *99*, 4312.
- (17) Tarroni, R.; Carter, S. *J. Chem. Phys.* **2003**, *119*, 12878.
- (18) Hsu, Y.-C.; Shiu, Y.-J.; Lin, C.-M. *J. Chem. Phys.* **1995**, *103*, 5919.
- (19) Zhou, J.; Garand, E.; Neumark, D. M. *J. Chem. Phys.* **2007**, *127*, 114313.
- (20) Taylor, R. T.; Xu, C.; Neumark, D. M. *J. Chem. Phys.* **1998**, *108*, 10018.
- (21) Brugh, D. L.; DaBell, R. S.; Morse, M. D. *J. Chem. Phys.* **2004**, *121*, 12379.
- (22) Loock, H.-P.; Bérces, A.; Simard, B.; Linton, C. *J. Chem. Phys.* **1997**, *107*, 2720.
- (23) Bopegedera, A. M. R. P.; Brazier, C. R.; Bernath, P. F. *Chem. Phys. Lett.* **1987**, *136*, 97.
- (24) Bopegedera, A. M. R. P.; Brazier, C. R.; Bernath, P. F. *J. Mol. Spectrosc.* **1988**, *129*, 268.
- (25) Nuccio, B. P.; Apponi, A. J.; Ziurys, L. M. *Chem. Phys. Lett.* **1995**, *247*, 283.
- (26) Anderson, M. A.; Ziurys, L. M. *Astrophys. J.* **1995**, *444*, L57.
- (27) Anderson, M. A.; Ziurys, L. M. *Astrophys. J.* **1995**, *439*, L25.
- (28) Brewster, M. A.; Apponi, A. J.; Xin, J.; Ziurys, L. M. *Chem. Phys. Lett.* **1999**, *310*, 411.
- (29) Fan, J.; Wang, L.-S. *J. Phys. Chem.* **1994**, *98*, 11814.
- (30) Moravec, V. D.; Jarrold, C. C. *J. Chem. Phys.* **2000**, *112*, 792.
- (31) Omae, I. *Appl. Organomet. Chem.* **2007**, *21*, 318.
- (32) Li, G. L.; Li, Q. S.; Xie, Y. M.; King, R. B.; Schaefer, H. F. *Organometallics* **2009**, *28*, 3390.
- (33) Ruppel, J. V.; Kamble, R. M.; Zhang, X. P. *Org. Lett.* **2007**, *9*, 4889.
- (34) Lumby, R. J. R.; Joensuu, P. M.; Lam, H. W. *Org. Lett.* **2007**, *9*, 4367.
- (35) Xu, H.-G.; Zhang, Z.-G.; Feng, Y.; Yuan, J. Y.; Zhao, Y. C.; Zheng, W. J. *Chem. Phys. Lett.* **2010**, *487*, 204.
- (36) Stephens, P. J.; Devlin, F. J.; Chabalowski, C. F.; Frisch, M. J. *J. Phys. Chem.* **1994**, *98*, 11623.
- (37) Becke, A. D. *Phys. Rev. A* **1988**, *38*, 3098.
- (38) Becke, A. D. *J. Chem. Phys.* **1993**, *98*, 5648.
- (39) Lee, C.; Yang, W.; Parr, R. G. *Phys. Rev. B* **1988**, *37*, 785.
- (40) Frisch, M. J.; Trucks, G. W.; Schlegel, H. B.; Scuseria, G. E.; Robb, M. A.; Cheeseman, J. R.; Zakrzewski, V. G.; Montgomery, J. A., Jr.; Stratmann, R. E.; Burant, J. C.; Dapprich, S.; Millam, J. M.; Daniels, A. D.; Kudin, K. N.; Strain, M. C.; Farkas, O.; Tomasi, J.; Barone, V.; Cossi, M.; Cammi, R.; Mennucci, B.; Pomelli, C.; Adamo, C.; Clifford, S.; Ochterski, J.; Petersson, G. A.; Ayala, P. Y.; Cui, Q.; Morokuma, K.; Malick, D. K.; Rabuck, A. D.; Raghavachari, K.; Foresman, J. B.; Cioslowski, J.; Ortiz, J. V.; Baboul, A. G.; Stefanov, B. B.; Liu, G.; Liashenko, A.; Piskorz, P.; Komaromi, I.; Gomperts, R.; Martin, R. L.; Fox, D. J.; Keith, T.; Al-Laham, M. A.; Peng, C. Y.; Nanayakkara, A.; Challacombe, M.; Gill, P. M. W.; Johnson, B.; Chen, W.; Wong, M. W.; Gonzalez, C.; Pople, J. A. *Gaussian 03*; Gaussian, Inc.: Wallingford, CT, 2004.
- (41) Li, X.; Wang, L.-S. *J. Chem. Phys.* **1999**, *111*, 8389.
- (42) Tono, K.; Terasaki, A.; Ohta, T.; Kondow, T. *J. Chem. Phys.* **2002**, *117*, 7010.
- (43) Dean, J. A. Properties of atoms, radicals, and bonds. *Lange's Handbook of Chemistry*; section 4, p 36.
- (44) Zhou, H.; Tamura, H.; Takami, S.; Kubo, M.; Belosludov, R.; Zhanpeisov, N.; Miyamoto, A. *Appl. Surf. Sci.* **2000**, *158*, 38.
- (45) Barden, C. J.; Rienstra-Kiracofe, J. C.; Schaefer, H. F. *J. Chem. Phys.* **2000**, *113*, 690.
- (46) Castro, M.; Jamorski, C.; Salahub, D. R. *Chem. Phys. Lett.* **1997**, *271*, 133.
- (47) Pereiro, M.; Baldomir, D.; Iglesias, M.; Rosales, C.; Castro, M. *Int. J. Quantum Chem.* **2001**, *81*, 422.
- (48) Datta, S.; Kabir, M.; Ganguly, S.; Sanyal, B.; Saha-Dasgupta, T.; Mookerjee, A. *Phys. Rev. B* **2007**, *76*, 014429.
- (49) Fan, H.-J.; Liu, C.-W.; Liao, M.-S. *Chem. Phys. Lett.* **1997**, *273*, 353.
- (50) Jamorski, C.; Martinez, A.; Castro, M.; Salahub, D. R. *Phys. Rev. B* **1997**, *55*, 10905.
- (51) Ma, Q.-M.; Xie, Z.; Wang, J.; Liu, Y.; Li, Y.-C. *Phys. Lett. A* **2006**, *358*, 289.
- (52) Sebetci, A. *Chem. Phys.* **2008**, *354*, 196.
- (53) Yoshida, H.; Terasaki, A.; Kobayashi, K.; Tsukada, M.; Kondow, T. *J. Chem. Phys.* **1995**, *102*, 5960.
- (54) Pereiro, M.; Man'kovsky, S.; Baldomir, D.; Iglesias, M.; Mlynarski, P.; Valladares, M.; Suarez, D.; Castro, M.; Arias, J. E. *Comput. Mater. Sci.* **2001**, *22*, 118.
- (55) Rodriguez-Lopez, J. L.; Aguilera-Granja, F.; Michaelian, K.; Vega, A. *Phys. Rev. B* **2003**, *67*, 174413.
- (56) Knickelbein, M. B. *J. Chem. Phys.* **2006**, *125*, 044308.